

# Redox and temperature-sensitive changes in microbial communities and soil chemistry dictate greenhouse gas loss from thawed permafrost

Jessica G. Ernakovich  · Laurel M. Lynch · Paul E. Brewer · Francisco J. Calderon · Matthew D. Wallenstein

Received: 1 March 2017 / Accepted: 22 June 2017  
© Springer International Publishing AG 2017

**Abstract** Greenhouse gas (GHG) emissions from thawed permafrost are difficult to predict because they result from complex interactions between abiotic drivers and multiple, often competing, microbial metabolic processes. Our objective was to characterize mechanisms controlling methane (CH<sub>4</sub>) and carbon dioxide (CO<sub>2</sub>) production from permafrost. We simulated permafrost thaw for the length of one growing season (90 days) in oxic and anoxic treatments at 1 and 15 °C to stimulate aerobic and anaerobic respiration. We measured headspace CH<sub>4</sub> and CO<sub>2</sub> concentrations, as well as soil chemical and biological

parameters (e.g. dissolved organic carbon (DOC) chemistry, microbial enzyme activity, N<sub>2</sub>O production, bacterial community structure), and applied an information theoretic approach and the Akaike information criterion to find the best explanation for mechanisms controlling GHG flux. In addition to temperature and redox status, CH<sub>4</sub> production was explained by the relative abundance of methanogens, activity of non-methanogenic anaerobes, and substrate chemistry. Carbon dioxide production was explained by microbial community structure and chemistry of the DOC pool. We suggest that models of permafrost CO<sub>2</sub> production are refined by a holistic view of the system, where the prokaryote community structure and detailed chemistry are considered. In contrast, although CH<sub>4</sub> production is the result of many syntrophic interactions, these actions can be

---

Responsible Editor: E. Matzner.

---

**Electronic supplementary material** The online version of this article (doi:[10.1007/s10533-017-0354-5](https://doi.org/10.1007/s10533-017-0354-5)) contains supplementary material, which is available to authorized users.

---

J. G. Ernakovich (✉)  
CSIRO Agriculture & Food, PMB 2 Waite Rd., Urrbrae,  
SA 5064, Australia  
e-mail: [jessica.ernakovich@gmail.com](mailto:jessica.ernakovich@gmail.com)

J. G. Ernakovich · L. M. Lynch · F. J. Calderon ·  
M. D. Wallenstein  
Natural Resource Ecology Laboratory, Colorado State  
University, 1499 Campus Delivery, Fort Collins,  
CO 80523, USA

L. M. Lynch  
Graduate Degree Program in Ecology, 1036 Campus  
Delivery Colorado State University, Fort Collins,  
CO 80523, USA

P. E. Brewer  
Smithsonian Environmental Research Center, 647  
Contees Wharf Rd, Edgewater, MD 21037, USA

F. J. Calderon  
USDA-ARS, Central Great Plains Research Station,  
40335 Co Rd GG, Akron, CO 80720, USA

M. D. Wallenstein  
Department of Ecosystem Science and Sustainability,  
Colorado State University, 1499 Campus Delivery,  
Fort Collins, CO 80523, USA

aggregated into a linear approach, where there is a single path of organic matter degradation and multiple conditions must be satisfied in order for methanogenesis to occur. This concept advances our mechanistic understanding of the processes governing anaerobic GHG flux, which is critical to understanding the impact the release of permafrost C will have on the global C cycle.

**Keywords** Greenhouse gas production · Information theoretic · Illumina sequencing · Fourier transform infrared (FTIR) spectroscopy · Methanogenesis · Microbial respiration

### Abbreviations

GHG	Greenhouse gas
CH <sub>4</sub>	Methane
CO <sub>2</sub>	Carbon dioxide
DOC	Dissolved organic carbon
IT	Information theoretic
AICc	Akaike information criterion
C	Carbon
ESM	Earth systems models
FTIR	Fourier transformed mid-infrared spectroscopy
PCoA	Principle coordinates analysis
ANOSIM	Analysis of similarity
PCA	Principle components analysis
MBC	Microbial biomass carbon

### Introduction

Permafrost soils contain vast stores of organic carbon (C) that are vulnerable to decomposition following thaw (Tarnocai et al. 2009; Harden et al. 2012; Schaedel et al. 2014). Rapid climate change at northern latitudes is causing widespread permafrost degradation (Vaughan et al. 2013) that could increase greenhouse gas (GHG) emissions and lead to a potential C-climate feedback (Anisimov 2007; MacDougall et al. 2012; Koven et al. 2015). The concentration of soil oxygen controls whether aerobic or anaerobic decomposition will occur following permafrost thaw, and geomorphology dictates whether soils are drained or inundated with water (Lipson et al. 2012; Elberling et al. 2013). Freely drained upland soils produce CO<sub>2</sub> as a result of aerobic respiration,

whereas saturated soils quickly become anoxic, favoring anaerobic processes such as denitrification, fermentation, iron or sulfate reduction, and methanogenesis. But, GHG production under anoxic conditions is hampered by the fact that anaerobic respiration yields less energy than aerobic respiration. Knoblauch et al. (2013) showed that only 25% of the C that was mineralized aerobically was mineralized under anaerobic conditions (to CO<sub>2</sub> and CH<sub>4</sub>) at 4 °C for 1200 days. The feedbacks and interactions between the mechanisms controlling the rate of GHG emission and the partitioning between CO<sub>2</sub> and CH<sub>4</sub> make it difficult to predict gaseous losses from thawed permafrost (Lee et al. 2012).

Permafrost C has been found to be particularly chemically labile (Coolen et al. 2011; Ernakovich et al. 2015) and susceptible to decomposition (Waldrop et al. 2010), which may in part be due to a lack of organo-mineral complexes and aggregate structure in permafrost soils (Höfle et al. 2013). Both aerobic and anaerobic metabolism are sensitive to the lability of organic matter (Hodgkins et al. 2014), however methanogenesis seems especially sensitive (Lupascu et al. 2012; Treat et al. 2015). Methane production is greater for soils with labile litter than those that are more chemically recalcitrant, such as *Sphagnum* moss litter (Lupascu et al. 2012) or partially-decomposed peat (Hodgkins et al. 2014). This may be due to the syntrophy of anaerobes required to break down organic matter to CH<sub>4</sub>, a process requiring the fermentation and depolymerization activities of microorganisms higher on the redox ladder to provide substrates, such as organic acids, for methanogenesis (Meronigal et al. 2003; Kotsyurbenko 2005; Drake et al. 2009).

The amount of GHG produced from thawed permafrost also depends on the activity and size of the decomposer biomass pool (Santruckova et al. 2003), and microbial community composition is increasingly recognized as another important driver of GHG flux from soils (Trivedi et al. 2013). Graham et al. (2016) recently found that including community structure in aerobic respiration models improved their explanatory power across a wide range of soil types. In anaerobic metabolism, relationships between microbial community composition and biogeochemistry appear to be highly correlated, as was observed for denitrification and sulfur cycling in oxygen minimum zones (Reed et al. 2014). In both laboratory induced-

and field based-permafrost thaw, methane flux has been correlated to the relative abundance of a single, recently—described methanogen, *Methanoflorens stordalenmirensis* (Mondav et al. 2014; McCalley et al. 2014; Hultman et al. 2015).

Models of GHG emissions from permafrost have advanced over the last decade, resolving soil depth, biogeochemistry, and ice content, as well as including an anaerobic fraction and gaseous diffusion (Lawrence et al. 2008; Koven et al. 2009; Swenson and Lawrence 2012), all of which are important in determining the type, rate, and magnitude of GHG emissions. However, a recent model synthesis identified the need to constrain CH<sub>4</sub> estimates from Earth system models (ESM), as they varied fivefold relative to a twofold variation in CO<sub>2</sub> emissions (McGuire et al. 2016). The authors also highlighted that only 4 of the 15 leading models included CH<sub>4</sub> components. Most C released from permafrost is CO<sub>2</sub> (Schädel et al. 2016), even under saturated soil conditions. However, CH<sub>4</sub> emissions exert a disproportionate effect on global climate owing to their higher radiative forcing (IPCC 2013). Thus, the partitioning between CO<sub>2</sub> and CH<sub>4</sub> is critical for modeling future climate. Because the degradation of plant and microbial polymers to CO<sub>2</sub> and CH<sub>4</sub> involves myriad microbial groups that produce and consume different intermediate substrates—each with their own intrinsic rates and limitations (Tveit et al. 2015)—including relevant biological and chemical controls in the models could be beneficial. While the complex interactions of ecosystem metabolism may be outside the scope of ecosystem-scale permafrost C models, we aim to provide simpler representations of chemical and biological constraints to refine GHG estimates from thawing permafrost.

The objective of this study was to determine potential mechanisms controlling methanogenesis and CO<sub>2</sub> production from freshly-thawed permafrost soil. We manipulated redox status to stimulate aerobic and anaerobic metabolism by allowing permafrost soil to drain or remain inundated when thawed and incubated soil at 1 and 15 °C for 90 days. We hypothesized that feedbacks between abiotic conditions (temperature and redox status), soil microorganisms, and soil chemistry govern CO<sub>2</sub> and CH<sub>4</sub> production. Specifically, we hypothesized that (1) incubation conditions would drive shifts in microbial community biomass and composition. In particular, we expected the relative abundance of methanogens

would correlate with methanogenesis, while a community-level approach would be appropriate for CO<sub>2</sub> production; (2) carbon dioxide production would not be correlated to any specific chemical functional group, but rather would be related to the total soil C, while CH<sub>4</sub> production would be correlated to the consumption of labile compounds, such as carbohydrates and organic acids; and (3) microbial activity would drive both CO<sub>2</sub> and CH<sub>4</sub> flux, while potential enzyme activities would be relevant for CO<sub>2</sub> flux and soil redox potential would be relevant for CH<sub>4</sub> production. We used an Information Theoretic Approach (IT) approach (Burnham and Anderson 2003) to test these a priori hypotheses about the effect of soil chemistry, microbial communities, and microbial activity on permafrost CH<sub>4</sub> and CO<sub>2</sub> production.

## Materials and methods

### Study site, soil sampling and processing

Fifteen permafrost cores were collected from Sagwon Hills, Alaska (N 69°25′32.190″ W 148°41′38.731″, 288 m above sea level) from a 150 m<sup>2</sup> grid on a north-facing slope under moist acidic tundra (MAT) vegetation in August 2009. MAT vegetation is dominated by tussock-forming grass (*Eriophorum vaginatum*), but also contains shrubs and sphagnum moss, which supports a thick, cryoturbated active layer (Borden et al. 2010; Soil Survey Staff, Natural Resources Conservation Service, United States Department of Agriculture 2015). The soils are classified as Ruptic Histic Aquiturbels, and are high in soil C (Supplementary Table 1) owing to their loess origin over gravel deposits (Borden et al. 2010). The depth to the permafrost surface was 26.8 ± 1.3 cm (determined by removing the active layer). At the time of sampling, the active layer was thawed through and we reached a frozen surface with 2–3 cm ice indicative of the permafrost boundary. Permafrost was collected from 0 to 10 cm below the frozen boundary, or approximately 27–37 cm below the surface of the vegetation. Permafrost soils were obtained as 8.0 cm diameter cores using a Tanaka auger fitted with a SIPRE-style (Snow, Ice, and Permafrost Research Establishment, Tarnocai 1993) soil corer with carbide bits (Jon's Machine Shop, Fairbanks, Alaska). A full description of the active layer and permafrost soil profile was

published previously (Ernakovich et al. 2015), and the site was previously described by Borden et al. 2010. For this study, we used the top ten centimeters of permafrost, which may be part of either the “transient” permafrost layer, owing to a chemical signature similar to the active layer (Ernakovich et al. 2015; Ping et al. 2015), or the “intermediate” permafrost layer owing to the observed ataxitic ice structure (Ping et al. 2015). According to Ping et al. 2015, these layers are both permafrost. The samples remained frozen during sampling, transportation, homogenization, and storage. Permafrost cores were scraped to remove contamination from active layer material then homogenized in a walk-in  $-10\text{ }^{\circ}\text{C}$  freezer by crushing the soils with a hammer while double-wrapped in sterile plastic bags inside autoclaved canvas bags. The samples were stored for 36 months at  $-10\text{ }^{\circ}\text{C}$  until incubation, well below the field temperature (average =  $-1\text{ }^{\circ}\text{C}$  at the time of sampling).

#### Incubation design and headspace gas analysis

We randomly assigned twelve soils (from the original 15) to either oxic or anoxic treatments ( $n = 6$ ), and then split them for incubation at 1 or  $15\text{ }^{\circ}\text{C}$  so that each of the four treatments had six replicates. Samples were placed inside 473 ml plastic containers (Silgan Plastics Corporation, Norcross, GA), which were then placed in 1.89 L glass jars with gas-tight metal lids fitted with two septa ports. As they thawed, samples in the oxic treatment lost water through holes drilled approximately every centimeter in the plastic containers; thus water from the oxic treatment freely drained. Anoxic samples had the same set-up, except that no holes were drilled in the plastic containers, so the samples were inundated with water after thaw. Samples in the anoxic treatment were not opened during the course of the incubation, and samples in the oxic treatment were opened once to remove drained water (at 5 days for the  $15\text{ }^{\circ}\text{C}$  samples and 10 days for the  $1\text{ }^{\circ}\text{C}$  samples). The incubation lasted 90 days, which we determined was the number of days the active layer was above  $0\text{ }^{\circ}\text{C}$  at this site between the years 2004–2008 (Soil Survey Staff, Natural Resources Conservation Service, United States Department of Agriculture 2015).

Cumulative gas production was determined by measuring headspace gas concentration on days 0, 1, 2, 3, 5, 8, 10, 16, 23, 30, 37, 44, 58, 71, and 90 to ensure

that headspace  $\text{CO}_2$  concentrations remained below 1.5%. Then jar headspace was replaced by flushing the jars (while closed through the two septa) for 20 min at  $4\text{ }^{\circ}\text{C}$  with  $\text{CO}_2$ -free air or with pure  $\text{N}_2$  gas for the oxic and anoxic treatments, respectively. Carbon dioxide concentrations were determined with a LI-COR 6525 infrared gas analyzer (LI-COR, Lincoln, Nebraska, USA) calibrated against a standard curve with a known  $\text{CO}_2$  concentration. Headspace  $\text{CH}_4$  and  $\text{N}_2\text{O}$  gas samples were analyzed with a hybrid gas chromatograph (GC)/laser spectroscopy (LS) system using standards of known  $\text{CH}_4$  and  $\text{N}_2\text{O}$  concentrations. At the time of  $\text{CO}_2$  concentration analysis, 30 ml of headspace gas was injected into evacuated 20 ml glass for later analysis on the GC/LS system. Nitrous oxide was quantified with an electron capture device in the GC (Shimadzu GC-14B), and  $\text{CH}_4$  was quantified on a LS that measures  $\text{CO}_2$ ,  $\text{CH}_4$ , and  $\text{H}_2\text{O}$  (Los Gatos Fast Greenhouse Gas Analyzer; Los Gatos Research, Inc., San Jose, California, USA). Gas vials were sampled with the assistance of an AOC-5000 Combi-PAL autosampler (CTC Analytics AG, Zwingen, Switzerland). GC and LS data were processed with EZStart 7.2.1 software (Shimadzu). Cumulative  $\text{CO}_2\text{-C}$ ,  $\text{CH}_4\text{-C}$ , and  $\text{N}_2\text{O-N}$  were determined by summing values for each time step over 90 days.

#### Chemical and biological analysis

Chemical and biological analyses were performed on frozen soil (“initial”, Table 1) at the initiation of the experiment and immediately after gas sampling on day 90 (“harvest”, Table 1). Soil water content was determined by weighing soils and drying them for 48 h at  $105\text{ }^{\circ}\text{C}$ . Combustible C and N was measured on dried ( $55\text{ }^{\circ}\text{C}$ ) and ground soils using a LECO TruSPEC elemental analyzer (Leco Corp., St. Joseph, MI). Pore water DOC and N was collected by spinning soil samples for 30 min at 2500 rpm through  $0.45\text{ }\mu\text{m}$  nylon spin filters (Grace Discovery, Bannockburn, IL) that had been pre-conditioned with deionized (DI) water ( $3 \times 5\text{ min @ }2500\text{ rpm}$ ). Pore water was frozen for approximately one month at  $-20\text{ }^{\circ}\text{C}$  until analysis for C and N content on a Total Organic Carbon Analyzer (Shimadzu Scientific Instruments, Inc.). Lyophilized pore water samples ( $1\text{ }\mu\text{g C: }1\text{ mg KBr}$ ) were scanned undiluted in the mid-infrared region on a Digilab FTS 7000 Fourier transform spectrometer (Varian, Inc., Palo Alto, CA) with a deuterated, Peltier-

**Table 1** AICc values for models explaining CO<sub>2</sub> and CH<sub>4</sub> flux from thawed permafrost soils

Model	AICc, CO <sub>2</sub>	AICc, CH <sub>4</sub>
GHG flux = $f$ (redox temp, random effects) [null model]	41.9	80
GHG flux = $f$ (chemistry, chemistry*redox, redox temp, random effects)		
Add soil C (log initial)	41.7	71.4
Or soil C (log harvest)	38.6	64.1
Or TOC (log initial)	39.9	69.9
Or TOC (log harvest)	35.6	65.1
Or PC 1 FTIR chem (harvest)	34.6	<b>53.8</b>
Or PC 2 FTIR chem (harvest)	<b>29.1</b>	60.6
Or ratio 1040/1620	31.6	63.5
Or RA carbohydrates (1040 cm <sup>-1</sup> )	31.5	64.1
Or RA organic acids (1754 cm <sup>-1</sup> )		<b>55.2</b>
GHG flux = $f$ (microbial size/composition, microbial size/composition*redox, redox temp, random effects)		
Add MBC (log initial)	31.1	45
Or MBC (log harvest)	35.3	68
Or PCo 1 Comm Comp	<b>27.2</b>	54.8
Or PCo 2 Comm Comp	29.3	51.7
Or RA methanogens		<b>43.2</b>
GHG flux = $f$ (microbial activity, microbial activity*redox, redox temp, random effects)		
Add PC 1 15C enzymes	<b>41.2</b>	
Or PC 1 Q10 enzymes	42.2	
Or N <sub>2</sub> O prod (log)		<b>43.6</b>
Or redox		84.9
Or change in TOC (log)	43.9	74.9
CO <sub>2</sub> flux = $f$ (chemistry, microbial size/composition, chemistry*redox, microbial size/composition*redox, redox temp, random effects)		
Chemistry = PC 2 FTIR, microbial size/composition = Pco 1 Comm Comp	<b>17.7</b>	
Chemistry = PC 2 FTIR, microbial size/composition = Pco 2 Comm Comp	21.8	
CH <sub>4</sub> flux = $f$ (chemistry, microbial size/composition, microbial activity, chemistry*redox, microbial size/composition*redox, microbial activity*redox, redox temp, random effects)		
Chemistry = RA organic acids, microbial size/composition = RA methanogens, microbial activity = N <sub>2</sub> O prod		<b>1</b>
Chemistry = PC 1 FTIR, microbial size/composition = RA methanogens, microbial activity = N <sub>2</sub> O prod		<b>0.9</b>
Chemistry = PC 1 FTIR, microbial size/composition = MBC, microbial activity = N <sub>2</sub> O prod		17
Chemistry = RA organic acids, microbial size/composition = MBC, microbial activity = N <sub>2</sub> O prod		6.9

Covariates describing chemistry, microbial size or composition, and microbial activity were compared to null models, accounting for incubation conditions. The day of sample set-up and sample core (nested within incubation treatment) were included as random effects. Covariates from each category that improved the model were tested as a combined model. “Initial” and “harvest” indicate parameters evaluated on frozen soil and after 90 days of incubation, respectively. “I” denotes main effects and interactions, “redox” and “temp” are the incubation treatments manipulating redox status (oxic or anoxic treatment) and temperature (1 or 15 °C). For the *chemistry covariates*, “Soil C” and “TOC” were pool sizes (mg C g dry weight soil<sup>-1</sup> or µg C g dry weight soil<sup>-1</sup>, respectively). To account for the holistic complexity of the DOC pool, “PC 1 [or 2] FTIR chem” represent the principal component analysis (PCA) of the FTIR spectra. The ratio of the carbohydrates (1040 cm<sup>-1</sup> in the FTIR spectrum) to carboxylates (1620 cm<sup>-1</sup>) was calculated. “RA carbohydrates” and “RA organic acids” represent the relative abundance (in the FTIR spectrum) of carbohydrates (1040 cm<sup>-1</sup>) and organic acids (1754 cm<sup>-1</sup>), respectively. For the *microbial size/composition covariates*, “MBC” was a pool size (µg C g dry weight soil<sup>-1</sup>). The microbial community composition was accounted for (PCo 1 [or 2] Comm Comp) by extracting the first or second principal coordinate (PCo) of the weighted Unifrac distance (16S rRNA gene). “RA methanogens” represents the relative abundance of OTUs assigned to methanogens in the OTU table of 16S rRNA genes. For the *microbial activity covariates*, “PC 1 enzymes” represents the spatial distribution of the samples after principal component analysis of six hydrolytic enzyme assays (performed at 15°C). “PC 1 Q<sub>10</sub> enzymes” represents the temperature sensitivity of the same enzyme assays performed at 1 and 15°C (on all samples regardless of incubation treatment temperature). The “change in TOC” is a measure of the reduction in pore water C content (µg C g dry weight soil<sup>-1</sup>). The N<sub>2</sub>O production, as a result of denitrification, was used as a proxy for the effect of the activity of microbes higher on the redox ladder in “N<sub>2</sub>O prod”. “Redox” served as an indicator for general anaerobic microbial activity. Models with the lowest AICc values for each category and for the combined models are indicated in bold

cooled, triglycine sulfate detector and KBr beam splitter. The spectrometer was fitted with a Pike AutoDIFF diffuse reflectance accessory (Pike Technologies, Madison, WI) and KBr was used as background. Spectra were obtained as pseudo-absorbance ( $\log [1/\text{Reflectance}]$ ) at  $4 \text{ cm}^{-1}$  resolution, with 64 co-added scans per spectrum from 4000 to  $400 \text{ cm}^{-1}$ . Duplicate scans of each sample were performed and averaged. Fourier transformed mid-infrared spectra (FTIR) were mean-centered before further analysis. We extracted the labile phosphate pool using anion exchange membrane (AEM) resins in a modified ascorbic acid method (DeForest et al. 2012). Two  $2 \times 6 \text{ cm}$  AEM strips, charged with  $0.5 \text{ M NaHCO}_3$ , were placed in a centrifuge tube with a 1:10 dilution of soil and deionized water and shaken for 4 h at 150 rpm. Anion exchange membrane strips were removed from the soil slurry and extracted with 25 ml of  $0.5 \text{ M HCl}$  for four hours. We determined resin P using the colorimetric Murphy-Riley molybdate solution, where absorbance was measured at 700 nm on a Tecan Infinite M200 microplate reader (Tecan Trading AG, Switzerland). The detection limit was  $0.5 \text{ mg l}^{-1}$ . Total iron was determined by digesting 0.5 g of soil with 10 ml each of nitric and perchloric acid in a Teflon beaker for 24 h. Next, 10 ml of hydrofluoric acid was added to the beaker and incubated at  $125 \text{ }^\circ\text{C}$  for 12 h. The residue was reconstituted with 10 ml of  $12 \text{ M HCl}$ , and the resulting digestate analyzed on an inductively coupled plasma (ICP)–atomic emission spectrometer (Perkin-Elmer 7300 DV). Ferrous iron was determined by extracting 0.5 g of soil with  $0.1 \text{ M HCl}$  and analyzing the extract by ICP, as above.

pH was measured in a 1:5 soil:DI water solution with a TTT85 Titrator (Radiometer, Copenhagen, Denmark) after stirring for 30 min. Soil redox potential was measured with a VWR symPHony epoxy combination redox electrode probe and Thermo Scientific Orion 3 Star meter. Three redox values were obtained unless they were highly variable and then five measurements were taken.

Microbial biomass was determined using the chloroform-slurry technique as described in Fierer and Schimel (2003). Briefly, 0.5 ml ethanol-free chloroform was shaken with 5 g wet weight soil in 30 ml  $0.5 \text{ M K}_2\text{SO}_4$  for 4 h, after which the chloroform was removed by bubbling with air. Unfumigated controls

were obtained by shaking 5 g wet weight soil in 30 ml  $0.5 \text{ M K}_2\text{SO}_4$  for 4 h. The C and N contents of the fumigated and unfumigated samples were analyzed with a Total Organic Carbon Analyzer (Shimadzu Scientific Instruments, Inc.). Microbial biomass carbon and nitrogen were determined by difference. Ammonium ( $\text{NH}_4^+$ ), nitrate ( $\text{NO}_3^-$ ) and total free amino acids (TFAA) were determined on the unfumigated controls by colorimetric and fluorometric microplate assays, as described in Darrouzet-Nardi & Weintraub, 2014. We extracted microbial P by removing the labile inorganic P pool using AEM resin strips as above. We fumigated one subsample with chloroform for one hour and stored the unfumigated control at  $1 \text{ }^\circ\text{C}$ . We added 30 ml of  $0.5 \text{ M NaHCO}_3$  to fumigated and control tubes and let them shake for 16 h at 150 rpm. Following this, we centrifuged samples at 1500 rpm for 30 min and analyzed total P by ICP with a detection limit of 0.01 ppm (Perkin Elmer 7300 DV ICP-AES). Potential activities of six hydrolytic extracellular enzymes ( $\beta$ -glucosidase, cellobiohydrolase, xylosidase, acid phosphomonoesterase, *N*-acetylglucosaminidase, or leucine-aminopeptidase) at 1 and  $15 \text{ }^\circ\text{C}$  (Wallenstein et al. 2009) were determined using fluorescently-labeled substrates [4-methylumbelliferyl (MUB)- $\beta$ -D-glucoside, 4-MUB- $\beta$ -D-cellobioside, 4-MUB- $\beta$ -D-xyloside, 4-MUB-phosphate, 4-MUB-*N*-acetyl- $\beta$ -D-glucosaminide, L-leucine-7-amino-4-methylcoumarin (MUC)] in a deep-well microplate assay (Wallenstein et al. 2009; Bell et al. 2013; Koyama et al. 2013). We homogenized 1.0 g of soil for 45 s with 91 ml of 50 mM sodium acetate buffer (pH 6.5) in a Waring blender. While slurries mixed on a stir plate, we added 800  $\mu\text{l}$  soil slurry and 200  $\mu\text{l}$  of 200  $\mu\text{M}$  fluorescing substrate to the sample assay wells. We prepared two standard plates by incubating our soil slurry with MUB and MUC in absence of the substrate. Plates were incubated at  $15 \text{ }^\circ\text{C}$  for 6 h and at  $1 \text{ }^\circ\text{C}$  for 24 h. Following incubation, we pipetted 5  $\mu\text{l}$  of  $0.5 \text{ N NaOH}$  to each sample, centrifuged the plates for three minutes at 1500 rpm ( $\sim 350 \times g$ ), and transferred 250  $\mu\text{l}$  from each well into black 96-well plates. We scanned the plates on a Tecan Infinite M200 microplate reader at an excitation wavelength of 365 nm and an emission wavelength of 450 nm (Tecan Trading AG, Switzerland). Data are presented as nmol activity/g dry soil/hour.  $Q_{10}$  was calculated as:

$$Q_{10} = \left( \frac{\text{activity at } 15^\circ\text{C}}{\text{activity at } 1^\circ\text{C}} \right)^{\frac{10}{(15-1)}} \quad (1)$$

Genomic DNA was extracted from the soils using the Power Soil DNA Isolation Kit (MoBio Laboratories, Carlsbad, CA) following the manufacturer's instructions. Bacterial and Archaeal community structure was analyzed using the protocol defined by Caporaso et al. (2011). Briefly, we amplified the F515/R806 (V4) portion of the 16S rRNA gene with a unique 12-bp Golay barcode (515F: 5'-GTGCCAG CMGCCGCGTAA-3'; 806R: 5'-GGACTACHVG GGTWTCTAAT-3') using PCR. PCR reactions contained 0.5  $\mu\text{l}$  (10  $\mu\text{M}$ ) of forward and 0.5  $\mu\text{l}$  (10  $\mu\text{M}$ ) reverse primer, 3  $\mu\text{l}$  template DNA (1 ng/ $\mu\text{l}$ ) and 22.5  $\mu\text{l}$  Platinum PCR SuperMix (Invitrogen, Carlsbad, CA). The samples were amplified in triplicate, cleaned using a PCR Cleanup kit (MoBio Laboratories, Carlsbad, CA) and pooled. One sample was omitted for sequencing due to unsuccessful amplification. Sequencing was performed on the Illumina MiSeq platform (Illumina, San Diego, CA). The UPARSE pipeline (Edgar 2013) was used to quality-filter the reads (quality scores lower than 16 were removed), trim them to 250 base pairs, discard singletons, cluster OTUs, and map reads to OTUs. OTUs were clustered by 97% similarity using USEARCH and the most abundant OTU was chosen as the representative OTU (Edgar 2010). Taxonomy was assigned using UCLUST (Edgar 2010) trained against GreenGenes (Werner et al. 2011; McDonald et al. 2011). The sequences were rarefied to 74,500. The beta diversity was determined using weighted UniFrac (Lozupone et al. 2007), and principle coordinates analysis (PCoA) was performed in Qiime. Analysis of similarity (ANOSIM) was performed on the UniFrac distance matrix in PRIMER v7 (Clarke and Gorley 2017). The relative abundance of methanogens was determined by identifying methanogenic taxa from the output of the command "summarize\_taxa.py" in Qiime.

### Statistical analysis and modeling

Statistical differences between treatments in the cumulative gas flux and soil characteristics were determined using analysis of variance (ANOVA) using a mixed effect model (PROC MIXED, SAS 9.3, Cary NC) with incubation conditions [temperature

and redox status (oxic vs. anoxic treatments)] as fixed effects, and day of sample set-up and sample core (nested within incubation treatment) as random effects. Principle Components Analysis (PCA) of the FTIR data was performed using *PLS Plus/IQ* software in GRAMS/AI Ver. 9.1 (Thermo Galactic, Salem, NH). A PCA of the enzyme activity at 15 °C and the  $Q_{10}$  of the enzyme activity (Eq. 1) was performed using PRIMER v7 (Clarke and Gorley 2017).

The contribution of variations in soil chemistry and microbiology to  $\text{CO}_2$  and  $\text{CH}_4$  production were examined in an Information Theoretic framework (Burnham and Anderson 2003) using mixed effects modeling (PROC MIXED, SAS 9.3 Cary, NC) to test our a priori hypotheses. We used an IT model selection approach, which is widely employed in ecological settings, to avoid model over parameterization and data dredging (Stephens et al. 2005). The combined models are not intended to indicate the absolute optimal model that could be constructed from our predictor sets but rather to indicate whether the factors from these different categories are complementary and whether there are major differences in model fit due to small differences in factor combinations. Prior to model building and selection, we examined the data for outliers and collinearity between covariates (Zuur et al. 2009). Cumulative  $\text{CO}_2$  and  $\text{CH}_4$  production were log transformed and other covariates were transformed as needed to satisfy the assumption of normality. Model fit was evaluated using the Akaike Information Criterion corrected for small sample sizes (AICc) where a smaller number is a better model fit (Hurvich and Tsai 1989; Cavanaugh 1997), and models with a difference in AICc less than 2 were considered similar (Burnham and Anderson 2003). We hypothesized that the model fit would improve by including parameters explaining soil chemistry, microbial community size or composition, and microbial activity in addition to accounting for the conditions manipulated in the experiment—incubation temperature and redox status (oxic or anoxic treatments), as in the "combined" model below:

$$\text{CO}_2 \text{ or } \text{CH}_4 \text{ flux} = f(\text{chemistry, microbial size/} \\ \text{composition, microbial activity, redox status,} \\ \text{temperature, chemistry*redox status, microbial size/} \\ \text{composition*redox status, microbial activity} \\ \text{*redox status, redox status*temperature, random effects})$$

where chemistry, microbial size/composition, microbial activity, redox status, and temperature were the main fixed effects; chemistry\*redox status, microbial size/composition\*redox status, microbial activity\*redox status, and redox status\*temperature were the interactions of the fixed effects; and the day of sample set-up and sample core (nested within incubation treatment) were random effects.

To select candidate covariates for the “combined” model, we grouped covariates into the categories “chemistry”, “microbial community size/composition”, and “microbial activity” (Table 1), and selected models from within the categories that provided the greatest reduction in the AICc relative to the null model, which was of the form:

$$\text{CO}_2 \text{ or CH}_4 \text{ flux} = f(\text{redox status, temperature, redox status*temperature, random effects})$$

## Results

### CO<sub>2</sub> and CH<sub>4</sub> production

At the end of 90 days, average cumulative CO<sub>2</sub> production was 30–450 times greater than CH<sub>4</sub> for the anoxic treatments, and 500–2500 times greater for the oxic treatments. Both temperature and redox status significantly affected the cumulative CO<sub>2</sub> produced ( $p < 0.01$ ), but the interaction term was not significant ( $p > 0.05$ ) (Fig. 1). There was a significant effect of the interaction between redox status and temperature for methanogenesis ( $p < 0.05$ ) because the CH<sub>4</sub> produced in the anoxic treatment was 23 times greater at 15 °C than 1 °C ( $p < 0.01$ ) and the CH<sub>4</sub> produced from the drained treatment at both 1 and 15 °C was similar to that of the anoxic treatment at 1 °C (average:  $0.73 \pm 0.22 \mu\text{g C g dws}^{-1}$ ;  $p > 0.05$ ). After 90 days of incubation, neither CO<sub>2</sub> nor CH<sub>4</sub> production had plateaued, even at 15 °C. Carbon dioxide production rates were highest during the initial incubation phase (Fig. 1, Supplementary Table 3). In contrast, the rates of methane production in the anoxic 15 °C treatment started low and increased with time (Fig. 1). During the 90 days, soils lost  $0.32 \pm 0.07$  and  $0.18 \pm 0.05\%$  of soil C in the oxic and anoxic treatments at 1 °C, and  $0.90 \pm 0.16$  and

$0.61 \pm 0.21\%$  of soil C in the oxic and anoxic treatments at 15 °C.

### Dissolved organic matter chemistry

The size of the soil C (SOC) pool did not change significantly over the course of the 90-day incubation and was not different for any of the treatments (Supplementary Tables 1, 3;  $p > 0.05$ ). The size of the dissolved organic C (DOC) pool declined by 70% over the course of the incubation for the samples incubated in the oxic treatment at 15 °C ( $p = 0.001$ ), but the decline was not significant for the other temperature and redox treatments ( $p > 0.05$ ) (Supplementary Fig. 1).

Despite the similarity in the size of the DOC pools, the constituents, as revealed with FTIR spectroscopy, differed depending on the incubation conditions (Fig. 2a, b). Soils in the oxic treatment contained peaks at 1640 and a shoulder at 1530 cm<sup>-1</sup> regardless of incubation temperature, while those in the anoxic treatment incubated at 1 °C had less pronounced features in this region. 1640 cm<sup>-1</sup> is indicative of either aromatic C=C and amide I bonds (Movasaghi et al. 2008), and 1530 cm<sup>-1</sup> is indicative of aromatic C=C stretch or C–H bending and/or amide II bonds (Haberhauer and Gerzabek 1999; Movasaghi et al. 2008; Parikh et al. 2014). Lacking the shoulder at 1530 cm<sup>-1</sup>, the anoxic treatment samples incubated at 15 °C had a broad peak at 1590 cm<sup>-1</sup>, indicative of amide II and/or phenyl C=C bonds (Movasaghi et al. 2008). The peak at 1390 cm<sup>-1</sup> is present in all the samples, but also present in blank KBr background. The oxic treatment samples incubated at 15 °C had a different distribution of peaks in the region between 1200 and 950 cm<sup>-1</sup> than the other incubation conditions, with peaks at 1200 cm<sup>-1</sup> (aliphatic O–H, C–OH stretch), 1130 (oligosaccharide-OH stretch), 1090 cm<sup>-1</sup> (C–O–C stretch, polysaccharide-OH stretch), and a small shoulder at 1040 cm<sup>-1</sup> (polysaccharide C–O–C, C–OH stretch) (Movasaghi et al. 2008; Parikh et al. 2014). In contrast, the oxic treatment samples incubated at 1 °C and the anoxic treatment samples incubated at 1 and 15 °C only have a defined peak at 1040 cm<sup>-1</sup> in this region. The ratio of carbohydrates to carboxylates (1040 cm<sup>-1</sup>: 1620 cm<sup>-1</sup>) is an indicator of the degree of decomposition, with lower values indicating more previous

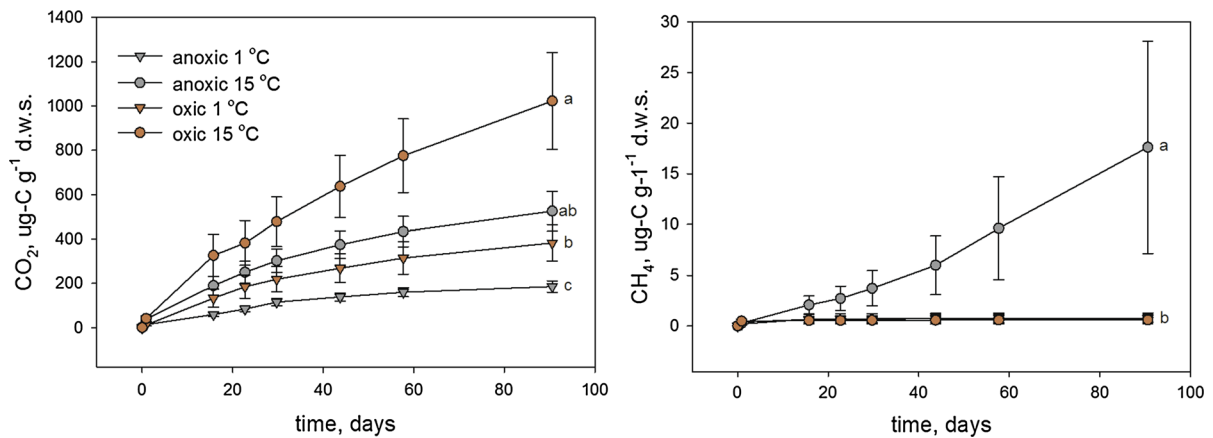


**Fig. 1** Average cumulative CO<sub>2</sub> (left) and CH<sub>4</sub> (right) production from mineral permafrost soil (0–10 cm below the frozen boundary or roughly 27–37 cm from the surface) in oxic and anoxic treatments during 90 days of incubation. Error bars are

one standard error of the mean. Letters indicate Tukey-adjusted significant differences ( $p < 0.05$ ) in cumulative gas flux at the final sampling point

decomposition (Artz et al. 2006). Microbial metabolism under both oxic and anoxic treatments at 15 °C resulted in 1.5 times less carbohydrates:carboxylates relative to 1 °C ( $p < 0.001$ ), but there was no significant difference in the ratio between redox conditions (Supplementary Fig. 2a).

Principal components analysis of the FTIR spectra further supported that the incubation resulted in differences in the chemical constituents (Fig. 2b). Samples in the oxic 15 °C treatment separated from the other samples along component 1 (PC 1; Fig. 2b). Analysis of the PC 1 loadings and the FTIR peak heights revealed that the oxic treatment samples incubated at 15 °C were depleted in polysaccharides relative to other incubation conditions (Fig. 2d, Supplementary Fig. 2b) and enriched in organic acids (Fig. 2c), carboxylates, aliphatics and non-cellulosic carbohydrates. Component 2 separated the incubation temperature for anoxic treatment samples, with the exception of two very active (e.g. high gas production) 1 °C samples, which clustered with the 15 °C samples, and one relatively inactive (e.g. low gas production) 15 °C sample, which clustered with the 1 °C samples; thus, high activity samples in the anoxic treatment—those with positive component 2 loadings—were relatively depleted of carbohydrates (including oligo-OH, poly-OH, and cellulose) and alcohols, but enriched in organic acids, carboxylates and phenyl C=C or amide II groups (Fig. 2d). Including specifics about the DOC chemistry resulted in a significant improvement to the AICc fit of the CO<sub>2</sub>

and CH<sub>4</sub> models (Table 1). PC 1 lowered the CO<sub>2</sub> model AICc from 41.9 (null) to 34.6, and the best chemistry model fit included PC 2 (29.1). Including PC 1 into the CH<sub>4</sub> model improved model fit (AICc from 80 (null) to 53.8).

The relative abundance of organic acids in the DOC was calculated by determining the peak height at 1754 cm<sup>-1</sup> relative to the nearest baseline (Hodgkins et al. 2014) (Fig. 2c). Soils in the oxic treatment had 60% more organic acid type absorbance than those in the anoxic treatment ( $p = 0.03$ ), indicating fermentation also occurred in the oxic treatments and organic acids accumulated (Fig. 2c, d). Organic acid abundance was low in the anoxic treatment, however the absence of both cellulosic and oligo- and poly-OH in the high activity anoxic samples (PC 2, Fig. 2d) suggests that fermentation of carbohydrates occurred. Including organic acids (i.e. peak height at 1754 cm<sup>-1</sup>) improved the CH<sub>4</sub> model (AICc: null = 80, null + organic acids = 55.2) but not the CO<sub>2</sub> model.

#### Microbial biomass size and community composition

Microbial biomass C was affected by the incubation conditions (Supplementary Fig. 3; redox status  $p = 0.0001$ , temperature  $p > 0.05$ , interaction  $p = 0.01$ ). Both microbial biomass N and P were unaffected by the redox condition ( $p > 0.05$ ), but the 15 °C treatment had over two times greater microbial

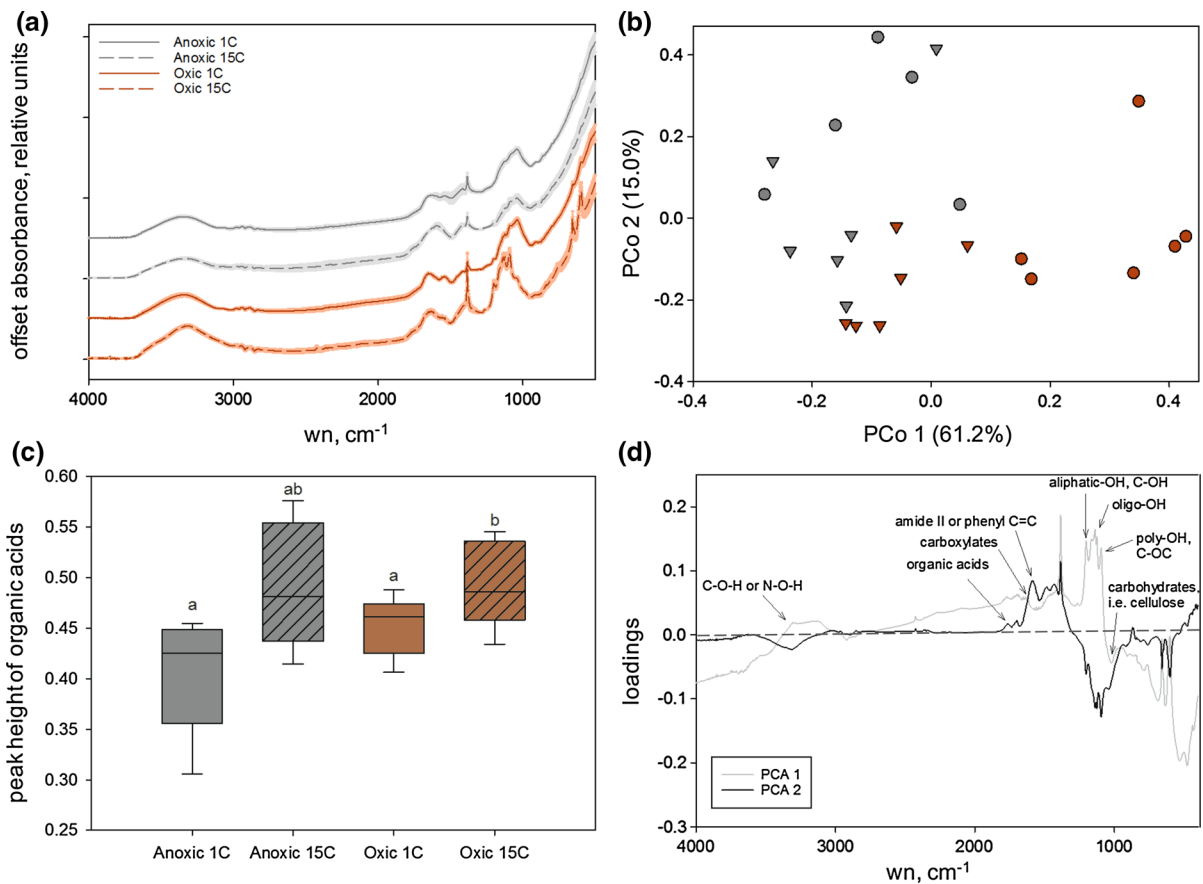


**Fig. 2** Dissolved organic matter chemistry. **a** Average FTIR spectra, **b** PCA after incubation in oxic (rust) and anoxic (grey) treatments at 1 (*triangle*) and 15 °C (*circle*), **c** boxplots of the peak heights at 1754 cm<sup>-1</sup> (organic acids), and **d** loadings of principal components. For the boxplots, the *solid line* is the median value, the *top* and *bottom* of the *boxes* represent the first and third quartiles, and the *whiskers* represent the extent of the data. The *letters* represent differences ( $p < 0.05$ ) of the mean

after a Tukey HSD multiple testing adjustment. For the loadings, PC 1 (*grey line*) separated the oxic 15 °C samples from the other samples, and wavenumbers with positive loading scores are important in the separation of those samples from the others in the PCA. PC 2 (*black line*) separated more active anoxic samples (positive loading scores) from less active (negative loading scores) ones

biomass N than the 1 °C treatment ( $p = 0.02$ ). Adding microbial biomass C to the models improved the fit of the CO<sub>2</sub> and CH<sub>4</sub> models, but did not provide the lowest AICc values (Table 1).

Analysis of the microbial community with ANOSIM revealed that incubation conditions structured the microbial community (temperature:  $R = 0.34$ ,  $p = 0.002$ ; redox status:  $R = 0.29$ ,  $p = 0.007$ ) (Fig. 3 a). The fit of the mixed effects model for CO<sub>2</sub> was improved by adding PCo 1 as a predictor in the model (AICc was reduced from 41.9 to 27.2). There was no significant effect of incubation treatment on the relative abundance of methanogens in the samples

(temperature, redox status, interaction:  $p > 0.05$ ), likely because of the large variability of samples incubated in the anoxic treatment. Although not significant, there is a decrease in the relative abundance in methanogens between the samples incubated at 1 versus 15 °C due to temperature driven changes in the community. Adding the relative abundance of methanogens to the model with incubation conditions improved the CH<sub>4</sub> model fit (AICc: null CH<sub>4</sub> model = 80; null + relative abundance methanogens = 43.2) driven by the positive correlation between the relative abundance of methanogens and CH<sub>4</sub> production in the anoxic treatment at 15 °C.

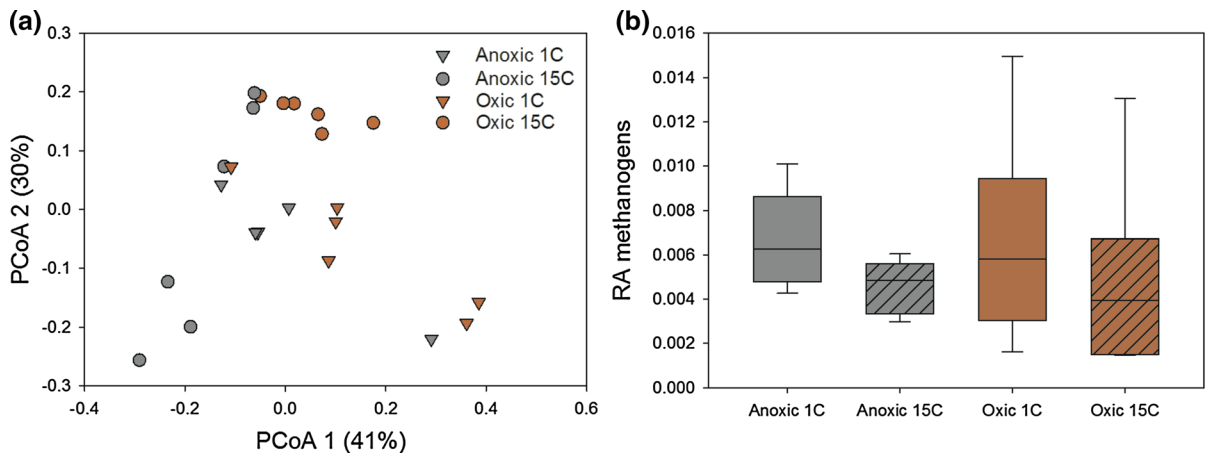


**Fig. 3** Bacterial community composition in the different incubation treatments, as assessed by Illumina MiSeq. **a** PCoA analysis of weighted UniFrac dissimilarity. Individual data-points are replicates. **b** Boxplots of the relative abundance (RA) of methanogens in the different incubation treatments. The *solid*

*line* is the median value, the *top* and *bottom* of the boxes represent the first and third quartiles, and the whiskers represent the extent of the data. There were no differences between the means for the RA of methanogens between treatments ( $p > 0.05$ )

### Microbial activity

There was no difference in enzyme activities or  $Q_{10}$  under the different incubation treatments (Supplementary Table 4 and Supplementary Fig. 4). Including enzyme activities in the model to explain the flux of  $CO_2$  from the incubations did not improve model fit (Table 1). Soil redox activity at the end of the incubation was spatially variable in some of the incubation jars (Fig. 4a). Soils incubated in the oxic treatment had redox values indicative of aerobic respiration or denitrification (approximately +300 mV). Samples incubated in the anoxic treatment at 15 °C generally had lower redox values than soils incubated at 1 °C, and soils with the lowest redox values produced the most  $CH_4$ . However, using soil redox as a covariate in the  $CH_4$  model did not improve model fit (Table 1).  $N_2O$  production from microcosms incubated in the anoxic treatment at 15 °C produced both the minimum and maximum  $N_2O$  observed (0.0–0.069  $\mu g N_2O-N/g$  dws), and there were no significant differences by treatment, however the redox status (oxic or anoxic) was nearly significant (temperature:  $p > 0.05$ ; redox status:  $p = 0.054$ ; interaction:  $p > 0.05$ ; Fig. 4b). Including cumulative  $N_2O$  production as a covariate in the  $CH_4$  model improved the model fit (AICc: null  $CH_4$  model = 80; null +  $N_2O$  model = 43.6).

### Combined models

Covariates resulting in the best fit for each of the categories (soil chemistry, microbial biomass size or composition, and microbial activity) were included in a combined model. For the  $CO_2$  model, none of the microbial activity covariates (enzyme activity, the  $Q_{10}$  of enzymes, and changes in DOC concentration) improved the model fit relative to the null model. Also, because the AICc values were within two of each other for the models using PCo 1 and PCo 2 (to represent community composition), combined models were tested with each. The best model fit for the  $CO_2$  flux included covariates for the chemistry of the DOC pool (PC 2 of FTIR) and community composition (PCo 1 of weighted UniFrac), and this model resulted in a reduction of the AICc from 41.9 for the null model to 17.7 (Table 1).

For  $CH_4$  flux, two models resulted in the “best” model fit. The first included the relative abundance of organic acids (peak height  $1754\text{ cm}^{-1}$ ), the relative abundance of methanogens, and  $N_2O$  production (AICc from 80 to 1.0). The other competing model included PC 1 of the FTIR chemistry rather than the relative abundance of organic acids (AICc 0.9). We also tested models with MBC because of competing AICc scores with the the relative abundance of methanogens, but these did not result in the best model fit (Table 1).

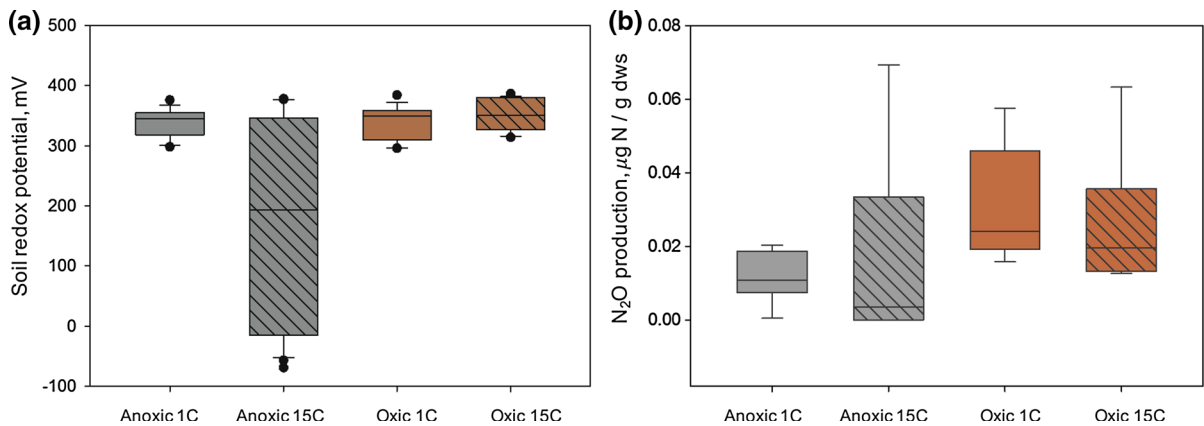


**Fig. 4** Boxplots of selected microbial activity parameters. For the soil redox potential (**a**), three to five measurements were taken for each jar at the end of the 90-day incubation and all data was included in the boxplot. **b** N<sub>2</sub>O production per gram dry weight soil from microcosms. Statistical differences were not detected between the N<sub>2</sub>O produced for different treatments (on

log transformed values). The *solid line* is the median value, the *top* and *bottom* of the *boxes* represent the first and third quartiles, and the *whiskers* extend 1.5 times the interquartile range from the 25th and 75th percentiles, *dots* represent samples that were greater than two standard deviations of the mean

## Discussion

The size to the permafrost C pool (Schuur et al. 2008; Tarnocai et al. 2009; Hugelius et al. 2014) and its bioavailability (Dutta et al. 2006; Waldrop et al. 2010; Lee et al. 2012; Ernakovich et al. 2015) make accurately estimating potential GHG emissions from thawing permafrost critical in understanding the global C-climate feedback. Current permafrost sub-models in ESMs use landscape position or other proxy of O<sub>2</sub> concentration to determine the form and magnitude of potential GHG emissions (Koven et al. 2011; Schuur et al. 2015; Lawrence et al. 2015). They implement scalars on aerobic respiration (Riley et al. 2011; Lawrence et al. 2015) or empirically-derived ratios of CO<sub>2</sub> and CH<sub>4</sub> (Koven et al. 2015) to partition between the two gases. However, accurately partitioning between these gases is complicated by the high spatial variability in CH<sub>4</sub> production across Arctic landscapes and under controlled laboratory conditions (Fig. 1; (Lee et al. 2012; Treat et al. 2015). If the mechanisms contributing to this variability were better represented in models, more accurate predictions of GHG flux from thawed permafrost could be made.

We found that accounting for microbial and soil chemical mechanisms can help explain variability in CO<sub>2</sub> and CH<sub>4</sub> flux from thawed permafrost. The incubation conditions (temperature and redox status) altered microbial community structure, biomass size,

and dissolved organic matter chemistry over the course of our 90-day incubation of permafrost soil. Permafrost CO<sub>2</sub> production was best explained by a holistic view of the microbial community and soil chemistry, where multivariate parameters improved the model fit. Methanogenesis was best explained by a series of positive and negative feedbacks between the relative abundance of methanogens, availability of organic acids or other labile substrates (i.e. carbohydrates), and the activity of other anaerobic processes (i.e. denitrification).

### A holistic approach to the explanation of CO<sub>2</sub> production

We found that CO<sub>2</sub> production was best explained by adding multivariate chemical and microbial parameters to the null model (containing only the incubation conditions), suggesting a holistic view of feedbacks between redox status, temperature, microbial community composition, and soil chemistry are appropriate. Carbon dioxide is the metabolic end-product of many different types of respiration—aerobic, denitrification, iron reduction, and so on through the redox ladder—and it dominates gaseous C loss from permafrost soils in both oxic and anoxic incubations (Schädel et al. 2016). The production of CO<sub>2</sub> was fueled by the consumption of carbohydrates and alcohols. Rapid depletion of carbohydrates in the initial stages of

decomposition is frequently observed in Arctic soils (Dai et al. 2002; Andersen and White 2006; Sjögersten et al. 2016). The supply of easily metabolized substrates like carbohydrates may be particularly important in permafrost soils, where low temperatures, anoxia, and nutrient availability might limit decomposition (Nadelhoffer et al. 1991; Melle et al. 2015; Wild et al. 2016). Samples producing more CO<sub>2</sub> also became enriched in phenyl C=C (lignin), carboxylates, and organic acids. Lignin accumulates in early stages of decomposition because bioavailable carbohydrates and alcohols are preferentially utilized (Cotrufo et al. 2015), and may accumulate in Arctic soils due to limitations on oxidative enzymes (Freeman et al. 2001). In contrast, carboxylates and organic acids are products of decomposition. Carboxylates accumulate over the course of decomposition (Artz et al. 2006) and through depth profiles (Haberhauer et al. 1998; Ernakovich et al. 2015), and organic acids are a product of fermentation (McInerney 1988). The production of both organic acids and N<sub>2</sub>O, the latter of which is a product of denitrification, is evidence that anaerobic metabolism occurred in our oxic treatments. We know of no other aerobic and anaerobic permafrost incubations that measured soil redox potential, but we observed redox potentials for most of our soils in the denitrification range (DeLaune and Reddy 2005). This suggests that freely drained permafrost will contain enough water to undergo some anaerobic metabolism, possibly in anoxic microsites (Groffman et al. 2009). However, the treatment differences in CO<sub>2</sub> production suggest aerobic metabolism still accounted for roughly half of the CO<sub>2</sub> lost in the oxic treatments.

Recent studies have observed rapid shifts in microbial community structure following thaw (Coolen et al. 2011; Mackelprang et al. 2011; Hultman et al. 2015) that are associated with shifts in function, from stress-dominated metabolism to the activation of metabolic pathways capable of degrading many different types of substrates (Frank-Fahle et al. 2014; Hultman et al. 2015; Coolen and Orsi 2015). We also observed that thawing conditions led to divergent microbial community structures, such that community-level information (PCo 1, which represents community similarity) improved the fit of the CO<sub>2</sub> model. In this model, differences among the microbial communities were quantified with weighted UniFrac scores, thus both the relative abundance and presence

of the taxa informed distances between samples in the PCoA (Lozupone et al. 2007). The observation that community similarity correlates strongly with CO<sub>2</sub> production within the constraints imposed by redox status and temperature suggests a link between phylogeny and ecosystem function generally not assumed for prokaryotes (but see Cleveland et al. 2013 and Graham et al. 2016). Whether this relationship between the environment and microbial community structure is causal or indirect cannot be ascertained in this experiment. Further work should explore whether the link between 16S amplicon data and CO<sub>2</sub> production is driven by changes in the richness or membership of the microbial community, and whether there are predictable links between certain members and CO<sub>2</sub> production in thawing permafrost. Ecosystem modelers now commonly use microbial community and chemistry data to create functional guilds to predict CO<sub>2</sub> production (Allison 2012; Tang and Riley 2013; Sistla et al. 2014; Wieder et al. 2015). The application of this approach to permafrost soils might be particularly powerful given our observation that multiple pathways of CO<sub>2</sub> production can occur simultaneously in freely-drained and saturated permafrost soils.

Greenhouse gas production is an end-product of microbial metabolism; thus, we posited that considering microbial activity rather than, or in addition to, community composition or size may be a successful and pragmatic tool for explaining CO<sub>2</sub> production. In the case of CO<sub>2</sub> production, we found that including covariates representing microbial activity parameters—such as soil enzymes and their temperature sensitivity or DOC changes—did not improve the fit beyond the null model with incubation conditions alone. While we utilized a suite of hydrolytic enzymes that are commonly used as a proxy for C-degrading enzymes, the reality is that they may poorly represent the diversity of enzymes involved in degrading the many C-rich substrates in soils (Wallenstein and Burns 2011). We also did not measure oxidative enzymes which have been shown to be particularly important for degrading of organic matter in mineral horizons of Arctic soils (Schnecker et al. 2014), but have methodological limitations. The collective activities of C-degrading enzymes represent only the first step in processes leading to respiration. Thus, they may provide a weak signal of the terminal step of respiratory processes, overwhelmed by the controls

exerted by microbial biomass, substrate-use efficiency, and physical controls on CO<sub>2</sub> diffusion from soils.

#### Linear approach to the explanation of methanogenesis

For CH<sub>4</sub> production, two models had low AICc scores, both of which included detailed chemical descriptions (either PC 1 of the FTIR or the relative amount of organic acids), the relative abundance of methanogens, and the activity of non-methanogenic anaerobes. Soils with high CH<sub>4</sub> production depleted carbohydrates, except intact polymeric carbohydrates (i.e. cellulose), relative to samples with low methanogenesis. This supports the notion that methanogenesis relies on substrate lability (Lupascu et al. 2012; Treat et al. 2015), however carbohydrates are not a substrate for methanogens directly. Rather, they are degraded in other anaerobic metabolic reactions, such as fermentation and acetogenesis, which supplies hydrogen or organic acids as substrates for methanogens (Peters and Conrad 1996; Megonigal et al. 2003). Heterotrophic methanogenesis using organic substrates is common in permafrost (Hodgkins et al. 2014; McCalley et al. 2014; Coolen and Orsi 2015), although rapid consumption and recycling of these substrates may make their detection difficult (van Hees et al. 2005; Drake et al. 2009) and methanogenesis can become substrate limited (Høj et al. 2006; Ganzert et al. 2007; Blake et al. 2015). Soils with lower levels of CH<sub>4</sub> production had relatively higher organic acid abundance than soils with higher levels of CH<sub>4</sub> production. These results suggest that methanogenesis was limited by substrate supply, which could be an important control on permafrost CH<sub>4</sub> fluxes.

Phylogenetic analysis of permafrost has revealed active methanogen populations (Rivkina et al. 2007; Waldrop et al. 2010; Mackelprang et al. 2011) that are governed by environmental factors, such as labile organic matter, water table depth, and soil redox status (Wachinger et al. 2000; Høj et al. 2006; Lupascu et al. 2012). The abundance of methanogens is correlated with rates of CH<sub>4</sub> production in permafrost (Wagner et al. 2007; Waldrop et al. 2010; Mackelprang et al. 2011). We found evidence that even the relative abundance has explanatory power, which was also found by McCalley et al. (2014). Thus, measuring methanogen relative abundance may be critically

important for predicting CH<sub>4</sub> efflux from thawed permafrost, in particular because the presence of this group is difficult to estimate by edaphic factors.

Methanogenesis has been described as the terminal reaction in the syntrophic degradation of plant material (Megonigal et al. 2003; Drake et al. 2009). In addition to the inhibitory effects on methanogenesis imposed by substrate supply, microorganisms higher on the redox ladder can impose energetic constraints on methanogenesis (Peters and Conrad 1996). For example, methanogenesis is thought to be suppressed in the presence of alternate electron acceptors that support higher energy yielding reactions, such as denitrification, iron reduction, and sulfate reduction (Bollag and Czlonkowski 1973; Westermann and Ahring 1987). Theoretical models claim that each of these reactions occurs in a narrow window of soil redox potential. Thus, we expected soil redox potential would indicate anaerobic microbial activity and explain CH<sub>4</sub> flux in our model. However, our measurements of soil redox potential were below the theoretical range of denitrification (DeLaune and Reddy 2005) only in the soils with high rates of methanogenesis, and including soil redox potential as a covariate did not help to explain CH<sub>4</sub> production. Rivkina et al. (2007) also observed CH<sub>4</sub> production and methanogen populations in permafrost with unexpectedly high redox potentials (30–212 mV). After observing CH<sub>4</sub> was produced in soils with redox potentials over +70 mV, Peters and Conrad (1996) posited that low redox potentials were an effect of, rather than a requirement for, methanogenesis. Although using redox potential as a general indicator of anaerobic activity did not improve the models, we did find a negative relationship between nitrous oxide production and methanogenesis, and including N<sub>2</sub>O production in the model lowered the AICc score. Denitrification, resulting in N<sub>2</sub>O production under anoxic conditions, is the most energetically efficient anaerobic metabolism, allowing denitrifiers to out-compete methanogens (Bollag and Czlonkowski 1973). Although the concept that the “redox ladder” and thermodynamics dictate favored decomposition pathways (i.e. that denitrification yields more energy and is therefore favored over iron reduction, which yields more energy and is therefore favored over methanogenesis) is not novel (Lovley and Phillips 1987), it is worth noting that this complexity is not currently incorporated into conceptual or

mathematical models of permafrost organic matter decomposition under anoxic conditions.

### Consequences for the terminal step in organic matter degradation

As permafrost thaws, the fate and final form of decomposing soil C will be determined by whether soils drain freely or remain saturated. However, this abiotic control only indicates which decomposition pathways are possible; from there, we need to consider the other mechanisms that promote or impede pathways of organic matter transformation. Rich bodies of literature describe mechanisms of methanogenesis and aerobic respiration in isolation, but only a handful of permafrost studies have tackled aerobic and anaerobic respiration together (Lee et al. 2012; Knoblauch et al. 2013; Treat et al. 2015). To our knowledge, we are the first to apply a hypothesis-driven modeling approach to define microbial and chemical controls on CO<sub>2</sub> and CH<sub>4</sub> production from permafrost in parallel. While both the CO<sub>2</sub> and CH<sub>4</sub> models benefited from the addition of microbial and chemical parameters, only the CO<sub>2</sub> models were improved by a holistic view of the chemistry and microbial community composition. In contrast, the CH<sub>4</sub> models were improved by including specific microbial groups (e.g. methanogens) and specific substrate types (e.g. organic acids). In addition, while the fit of the CH<sub>4</sub> model was improved by including a parameter for microbial activity (e.g. N<sub>2</sub>O production), microbial activity did not improve CO<sub>2</sub> models. This study highlights the need to mechanistically incorporate the microbial and chemical processes governing both aerobic and anaerobic respiration in drained and saturated permafrost soils after thaw; this will increase understanding and improve our predictions of GHG flux and resulting C-climate feedbacks.

**Acknowledgements** Jessica Ernakovich was funded by generous support from the National Science Foundation (Graduate Research Fellowship Program and Doctoral Dissertation Improvement Grant) and the Department of Energy Global Change Education Program Fellowship. Matthew Wallenstein was supported by Award Number 0902030 from the National Science Foundation Office of Polar Programs and an NSF CAREER Award (#1255228). This material is also based upon work supported by the U.S. Department of Energy, Office of Science, Office of Terrestrial Ecosystem Science, Award Number DE-SC0010568. Many thanks to Rachel Paige and Claire Freeman for assistance with

laboratory measures, and to Guy Beresford for the preparation of molecular libraries. Early discussions with J. Megan Steinweg, Sarah Evans and Joe vonFisher had a significant impact on the direction of this work. We would also like to thank the three anonymous reviewers and the editor for the time taken during review, as their comments significantly improved the manuscript.

**Disclaimer** The use of trade, firm, or corporation names is for the information and convenience of the reader. Such use does not constitute an official endorsement or approval by the United States Department of Agriculture or the Agricultural Research Service of any product or service to the exclusion of others that may be suitable. The U.S. Department of Agriculture (USDA) prohibits discrimination in all its programs and activities on the basis of race, color, national origin, age, disability, and where applicable, sex, marital status, familial status, parental status, religion, sexual orientation, genetic information, political beliefs, reprisal, or because all or part of an individual's income is derived from any public assistance program.

### References

- Allison SD (2012) A trait-based approach for modelling microbial litter decomposition. *Ecol Lett* 15:1058–1070. doi:10.1111/j.1461-0248.2012.01807.x
- Andersen SK, White DM (2006) Determining soil organic matter quality under anaerobic conditions in arctic and subarctic soils. *Cold Reg Sci Technol* 44:149–158. doi:10.1016/j.coldregions.2005.11.001
- Anisimov OA (2007) Potential feedback of thawing permafrost to the global climate system through methane emission. *Environ Res Lett*. doi:10.1088/1748-9326/2/4/045016
- Artz RR, Chapman SJ, Campbell CD (2006) Substrate utilisation profiles of microbial communities in peat are depth dependent and correlate with whole soil FTIR profiles. *Soil Biol Biochem* 38:2958–2962. doi:10.1016/j.soilbio.2006.04.017
- Bell CW, Fricks BE, Rocca JD et al (2013) High-throughput fluorometric measurement of potential soil extracellular enzyme activities. *JoVE*. doi:10.3791/50961
- Blake LI, Tveit A, Øvreås L et al (2015) Response of methanogens in arctic sediments to temperature and methanogenic substrate availability. *PLoS ONE* 10:e0129733. doi:10.1371/journal.pone.0129733
- Bollag JM, Czlonkowski ST (1973) Inhibition of methane formation in soil by various nitrogen-containing compounds. *Soil Biol Biochem* 5:673–678. doi:10.1016/0038-0717(73)90057-6
- Borden PW, Ping C-L, McCarthy PJ, Naidu S (2010) Clay mineralogy in arctic tundra Gelisols, northern Alaska. *Soil Sci Soc Am J* 74:580–592. doi:10.2136/sssaj2009.0187
- Burnham KP, Anderson DR (2003) Model selection and multimodel inference: a practical information-theoretic approach. pp 1–515
- Caporaso JG, Lauber CL, Walters WA et al (2011) Global patterns of 16S rRNA diversity at a depth of millions of sequences per sample. In: *Proceedings of the National*

- Academy of Sciences, vol 108 (Suppl 1), pp 4516–4522. doi:[10.1073/pnas.1000080107](https://doi.org/10.1073/pnas.1000080107)
- Cavanaugh JE (1997) Unifying the derivations for the Akaike and corrected Akaike information criteria. *Stat Prob Lett* 33:201–208
- Clarke KR, Gorley RN (2017) PRIMER v7, 3rd edn. Plymouth
- Cleveland CC, Reed SC, Keller AB et al (2013) Litter quality versus soil microbial community controls over decomposition: a quantitative analysis. *Oecologia* 174:283–294. doi:[10.1007/s00442-013-2758-9](https://doi.org/10.1007/s00442-013-2758-9)
- Coolen M, Orsi WD (2015) The transcriptional response of microbial communities in thawing Alaskan permafrost soils. *Front Microbiol* 1–14. doi:[10.3389/fmicb.2015.00197](https://doi.org/10.3389/fmicb.2015.00197)
- Coolen MJL, van de Giessen J, Zhu EY, Wuchter C (2011) Bioavailability of soil organic matter and microbial community dynamics upon permafrost thaw. *Environ Microbiol* 13:2299–2314. doi:[10.1111/j.1462-2920.2011.02489.x](https://doi.org/10.1111/j.1462-2920.2011.02489.x)
- Cotrufo MF, Soong JL, Horton AJ et al (2015) Formation of soil organic matter via biochemical and physical pathways of litter mass loss. *Nat Geosci* 8:776–779. doi:[10.1038/ngeo2520](https://doi.org/10.1038/ngeo2520)
- Dai XY, White D, Ping CL (2002) Comparing bioavailability in five Arctic soils by pyrolysis-gas chromatography/mass spectrometry. *J Anal Appl Pyrol* 62:249–258
- Darrouzet-Nardi A, Weintraub MN (2014) Evidence for spatially inaccessible labile N from a comparison of soil core extractions and soil pore water lysimetry. *Soil Biol Biochem* 73:22–32. doi:[10.1016/j.soilbio.2014.02.010](https://doi.org/10.1016/j.soilbio.2014.02.010)
- DeForest JL, Smemo KA, Burke DJ, Elliott HL (2012) Soil microbial responses to elevated phosphorus and pH in acidic temperate deciduous forests. *Biogeochemistry*. doi:[10.1007/s10533-011-9619-6](https://doi.org/10.1007/s10533-011-9619-6)
- DeLaune RD, Reddy KR (2005) Redox potential. *Encycl Soils Environ* 3:366–371
- Drake HL, Horn MA, Wüst PK (2009) Intermediary ecosystem metabolism as a main driver of methanogenesis in acidic wetland soil. *Environ Microbiol* 1:307–318. doi:[10.1111/j.1758-2229.2009.00050.x](https://doi.org/10.1111/j.1758-2229.2009.00050.x)
- Dutta K, Schuur EAG, Neff JC, Zimov SA (2006) Potential carbon release from permafrost soils of Northeastern Siberia. *Glob Change Biol* 12:2336–2351. doi:[10.1111/j.1365-2486.2006.01259.x](https://doi.org/10.1111/j.1365-2486.2006.01259.x)
- Edgar RC (2010) Search and clustering orders of magnitude faster than BLAST. *Bioinformatics* 26:2460–2461. doi:[10.1093/bioinformatics/btq461](https://doi.org/10.1093/bioinformatics/btq461)
- Edgar RC (2013) UPARSE: highly accurate OTU sequences from microbial amplicon reads. *Nat Methods* 10:996–998. doi:[10.1038/nmeth.2604](https://doi.org/10.1038/nmeth.2604)
- Elberling B, Michelsen A, Schädel C et al (2013) Long-term CO<sub>2</sub> production following permafrost thaw. *Nat Clim Change* 3:890–894. doi:[10.1038/nclimate1955](https://doi.org/10.1038/nclimate1955)
- Ernakovich JG, Wallenstein MD, Calderón FJ (2015) Chemical indicators of cryoturbation and microbial processing throughout an Alaskan permafrost soil depth profile. *Soil Sci Soc Am J* 79:783–793. doi:[10.2136/sssaj2014.10.0420](https://doi.org/10.2136/sssaj2014.10.0420)
- Fierer N, Schimel JP (2003) A proposed mechanism for the pulse in carbon dioxide production commonly observed following the rapid rewetting of a dry soil. *Soil Sci Soc Am J* 67:798–805
- Frank-Fahle BA, Yergeau E, Greer CW et al (2014) Microbial functional potential and community composition in permafrost-affected soils of the NW Canadian Arctic. *PLoS ONE* 9:e84761. doi:[10.1371/journal.pone.0084761](https://doi.org/10.1371/journal.pone.0084761)
- Freeman C, Ostle N, Kang H (2001) An enzymic “latch” on a global carbon store—a shortage of oxygen locks up carbon in peatlands by restraining a single enzyme. *Nature* 409:149. doi:[10.1038/35051650](https://doi.org/10.1038/35051650)
- Ganzert L, Jurgens G, Münster U, Wagner D (2007) Methanogenic communities in permafrost-affected soils of the Laptev Sea coast, Siberian Arctic, characterized by 16S rRNA gene fingerprints. *FEMS Microbiol Ecol* 59:476–488. doi:[10.1111/j.1574-6941.2006.00205.x](https://doi.org/10.1111/j.1574-6941.2006.00205.x)
- Graham EB, Knelman JE, Schindlbacher A (2016) Microbes as engines of ecosystem function: when does community structure enhance predictions of ecosystem processes? *Front Microbiol* 1–10. doi:[10.3389/fmicb.2016.00214](https://doi.org/10.3389/fmicb.2016.00214)
- Groffman PM, Butterbach-Bahl K, Fulweiler RW et al (2009) Challenges to incorporating spatially and temporally explicit phenomena (hotspots and hot moments) in denitrification models. *Biogeochemistry* 93:49–77. doi:[10.1007/s10533-008-9277-5](https://doi.org/10.1007/s10533-008-9277-5)
- Haberhauer G, Gerzabek MH (1999) Drift and transmission FT-IR spectroscopy of forest soils: an approach to determine decomposition processes of forest litter. *Vib Spectrosc* 19:413–417. doi:[10.1016/S0924-2031\(98\)00046-0](https://doi.org/10.1016/S0924-2031(98)00046-0)
- Haberhauer G, Rafferty B, Strebl F, Gerzabek MH (1998) Comparison of the composition of forest soil litter derived from three different sites at various decompositional stages using FTIR spectroscopy. *Geoderma* 83:331–342. doi:[10.1016/S0016-7061\(98\)00008-1](https://doi.org/10.1016/S0016-7061(98)00008-1)
- Harden JW, Koven CD, Ping C-L et al (2012) Field information links permafrost carbon to physical vulnerabilities of thawing. *Geophys Res Lett* 39:1–6. doi:[10.1029/2012GL051958](https://doi.org/10.1029/2012GL051958)
- Hodgkins SB, Tfaily MM, McCalley CK et al (2014) Changes in peat chemistry associated with permafrost thaw increase greenhouse gas production. *Proc Natl Acad Sci USA* 111:5819–5824. doi:[10.1073/pnas.1314641111](https://doi.org/10.1073/pnas.1314641111)
- Höfle S, Rethemeyer J, Mueller CW, John S (2013) Organic matter composition and stabilization in a polygonal tundra soil of the Lena Delta. *Biogeosciences* 10:3145–3158. doi:[10.5194/bg-10-3145-2013](https://doi.org/10.5194/bg-10-3145-2013)
- Høj L, Rusten M, Haugen LE, Olsen RA (2006) Effects of water regime on archaeal community composition in Arctic soils. *Environ Microbiol*. doi:[10.1111/j.1462-2920.2005.00982.x](https://doi.org/10.1111/j.1462-2920.2005.00982.x)
- Hugelius G, Strauss J, Zubrzycki S, Harden JW (2014) Estimated stocks of circumpolar permafrost carbon with quantified uncertainty ranges and identified data gaps. *Biogeosciences*. doi:[10.5194/bg-11-6573-2014](https://doi.org/10.5194/bg-11-6573-2014)
- Hultman J, Waldrop MP, Mackelprang R et al (2015) Multi-omics of permafrost, active layer and thermokarst bog soil microbiomes. *Nature*. doi:[10.1038/nature14238](https://doi.org/10.1038/nature14238)
- Hurvich CM, Tsai CL (1989) Regression and time-series model selection in small samples. *Biometrika* 76:297–307. doi:[10.1016/S0167-7152\(96\)00128-9](https://doi.org/10.1016/S0167-7152(96)00128-9)
- IPCC (2013) Climate change 2013: the physical science basis. In: Stocker TF, Qin D, Plattner GK, Tignor M, Allen SK, Boschung J, Nauels A, Xia Y, Bex V, Midgley PM (eds) Contribution of working group I to the fifth assessment

- report of the intergovernmental panel on climate change. Cambridge University Press, Cambridge, 1535 pp
- Knoblauch C, Beer C, Sosnin A et al (2013) Predicting long-term carbon mineralization and trace gas production from thawing permafrost of Northeast Siberia. *Glob Change Biol* 19:1160–1172. doi:[10.1111/gcb.12116](https://doi.org/10.1111/gcb.12116)
- Kotsyurbenko OR (2005) Trophic interactions in the methanogenic microbial community of low-temperature terrestrial ecosystems. *FEMS Microbiol Ecol* 53:3–13. doi:[10.1016/j.femsec.2004.12.009](https://doi.org/10.1016/j.femsec.2004.12.009)
- Koven C, Friedlingstein P, Ciais P et al (2009) On the formation of high-latitude soil carbon stocks: Effects of cryoturbation and insulation by organic matter in a land surface model. *Geophys Res Lett* 36:L21501–L21505. doi:[10.1029/2009GL040150](https://doi.org/10.1029/2009GL040150)
- Koven CD, Ringeval B, Friedlingstein P et al (2011) Permafrost carbon-climate feedbacks accelerate global warming. *Proc Natl Acad Sci USA* 108:14769–14774. doi:[10.1073/pnas.1103910108](https://doi.org/10.1073/pnas.1103910108)
- Koven CD, Schuur E, Schädel C (2015) A simplified, data-constrained approach to estimate the permafrost carbon-climate feedback. *R Soc A*. doi:[10.1098/rsta.2014.0423](https://doi.org/10.1098/rsta.2014.0423)
- Koyama A, Wallenstein MD, Simpson RT, Moore JC (2013) Carbon-degrading enzyme activities stimulated by increased nutrient availability in arctic tundra soils. *PLoS ONE* 8:e77212–e77213. doi:[10.1371/journal.pone.0077212](https://doi.org/10.1371/journal.pone.0077212)
- Lawrence DM, Slater AG, Romanovsky VE, Nicolsky DJ (2008) Sensitivity of a model projection of near-surface permafrost degradation to soil column depth and representation of soil organic matter. *J Geophys Res* 113:F02011–F02014. doi:[10.1029/2007JF000883](https://doi.org/10.1029/2007JF000883)
- Lawrence DM, Koven CD, Swenson SC et al (2015) Permafrost thaw and resulting soil moisture changes regulate projected high-latitude CO<sub>2</sub> and CH<sub>4</sub> emissions. *Environ Res Lett* 10:094011–094012. doi:[10.1088/1748-9326/10/9/094011](https://doi.org/10.1088/1748-9326/10/9/094011)
- Lee H, Schuur EAG, Inglett KS et al (2012) The rate of permafrost carbon release under aerobic and anaerobic conditions and its potential effects on climate. *Glob Change Biol* 18:515–527. doi:[10.1111/j.1365-2486.2011.02519.x](https://doi.org/10.1111/j.1365-2486.2011.02519.x)
- Lipson DA, Zona D, Raab TK et al (2012) Water-table height and microtopography control biogeochemical cycling in an Arctic coastal tundra ecosystem. *Biogeosciences* 9:577–591. doi:[10.5194/bg-9-577-2012](https://doi.org/10.5194/bg-9-577-2012)
- Lovley DR, Phillips EJP (1987) Competitive mechanisms for inhibition of sulfate reduction and methane production in the zone of ferric iron reduction in sediments. *Appl Environ Microbiol* 53:2636–2641
- Lozupone CA, Hamady M, Kelley ST, Knight R (2007) Quantitative and qualitative beta diversity measures lead to different insights into factors that structure microbial communities. *Appl Environ Microbiol* 73:1576–1585. doi:[10.1128/AEM.01996-06](https://doi.org/10.1128/AEM.01996-06)
- Lupascu M, Wadham JL, Hornibrook ERC, Pancost RD (2012) Temperature sensitivity of methane production in the permafrost active layer at Stordalen, Sweden: a comparison with non-permafrost Northern Wetlands. *Arct Antarct Alp Res* 44:469–482. doi:[10.1657/1938-4246-44.4.469](https://doi.org/10.1657/1938-4246-44.4.469)
- MacDougall AH, Avis CA, Weaver AJ (2012) Significant contribution to climate warming from the permafrost carbon feedback. *Nat Geosci* 5:719–721. doi:[10.1038/ngeo1573](https://doi.org/10.1038/ngeo1573)
- Mackelprang R, Waldrop MP, DeAngelis KM et al (2011) Metagenomic analysis of a permafrost microbial community reveals a rapid response to thaw. *Nature* 480:368–371. doi:[10.1038/nature10576](https://doi.org/10.1038/nature10576)
- McCalley CK, Woodcroft Ben J, Hodgkins SB et al (2014) Methane dynamics regulated by microbial community response to permafrost thaw. *Nature* 514:478–481. doi:[10.1038/nature13798](https://doi.org/10.1038/nature13798)
- McDonald D, Price MN, Goodrich J et al (2011) An improved Greengenes taxonomy with explicit ranks for ecological and evolutionary analyses of bacteria and archaea. *ISME J* 6:610–618. doi:[10.1038/ismej.2011.139](https://doi.org/10.1038/ismej.2011.139)
- McGuire AD, Koven C, Lawrence DM (2016) Variability in the sensitivity among model simulations of permafrost and carbon dynamics in the permafrost region between 1960 and 2009. *Global Biogeochem Cycles*. doi:[10.1002/\(ISSN\)1944-9224](https://doi.org/10.1002/(ISSN)1944-9224)
- McInerney MJ (1988) Anaerobic hydrolysis and fermentation of fats and proteins. In: Zehnder AJB (ed) *Biology of Anaerobic Microorganisms*. Wiley, New York, pp 373–415
- Megonigal JP, Hines ME, Visscher PT (2003) 8.08 anaerobic metabolism: linkages to trace gases and aerobic processes. In: Holland HD, Turekian KK (eds) *Treatise on geochemistry*. Elsevier-Pergamon, Oxford, pp 317–424
- Melle C, Wallenstein M, Darrouzet-Nardi A, Weintraub MN (2015) Microbial activity is not always limited by nitrogen in Arctic tundra soils. *Soil Biol Biochem* 90:52–61. doi:[10.1016/j.soilbio.2015.07.023](https://doi.org/10.1016/j.soilbio.2015.07.023)
- Mondav R, Woodcroft Ben J, Kim E-H et al (2014) Discovery of a novel methanogen prevalent in thawing permafrost. *Nat Commun* 5:1–7. doi:[10.1038/ncomms4212](https://doi.org/10.1038/ncomms4212)
- Movasaghi Z, Rehman S, ur Rehman DI (2008) Fourier transform infrared (FTIR) spectroscopy of biological tissues. *Appl Spectrosc Rev* 43:134–179. doi:[10.1080/05704920701829043](https://doi.org/10.1080/05704920701829043)
- Nadelhoffer KJ, Giblin AE, Shaver GR, Laundre JA (1991) Effects of temperature and substrate quality on element mineralization in six arctic soils. *Ecology* 72:242–253. doi:[10.2307/1938918](https://doi.org/10.2307/1938918)
- Parikh SJ, Goyne KW, Margenot AJ et al (2014) Soil chemical insights provided through vibrational spectroscopy. Elsevier, Oxford, pp 1–148
- Peters V, Conrad R (1996) Sequential reduction processes and initiation of CH<sub>4</sub> production upon flooding of oxic upland soils. *Soil Biol Biochem* 28:371–382. doi:[10.1016/0038-0717\(95\)00146-8](https://doi.org/10.1016/0038-0717(95)00146-8)
- Ping CL, Jastrow JD, Jorgenson MT et al (2015) Permafrost soils and carbon cycling. *Soil* 1:147–171. doi:[10.5194/soil-1-147-2015](https://doi.org/10.5194/soil-1-147-2015)
- Reed DC, Algar CK, Huber JA, Dick GJ (2014) Gene-centric approach to integrating environmental genomics and biogeochemical models. *Proc Natl Acad Sci USA* 111:1879–1884. doi:[10.1073/pnas.1313713111](https://doi.org/10.1073/pnas.1313713111)
- Riley WJ, Subin ZM, Lawrence DM et al (2011) Barriers to predicting changes in global terrestrial methane fluxes: analyses using CLM4Me, a methane biogeochemistry model integrated in CESM. *Biogeosciences* 8:1925–1953. doi:[10.5194/bg-8-1925-2011](https://doi.org/10.5194/bg-8-1925-2011)
- Rivkina E, Shcherbakova V, Laurinavichius K et al (2007) Biogeochemistry of methane and methanogenic archaea in

- permafrost. *FEMS Microbiol Ecol* 61:1–15. doi:[10.1111/j.1574-6941.2007.00315.x](https://doi.org/10.1111/j.1574-6941.2007.00315.x)
- Santruckova H, Bird MI, Kalaschnikov YN et al (2003) Microbial characteristics of soils on a latitudinal transect in Siberia. *Glob Change Biol* 9:1106–1117. doi:[10.1046/j.1365-2486.2003.00596.x](https://doi.org/10.1046/j.1365-2486.2003.00596.x)
- Schädel C, Bader MKF, Schuur EAG et al (2016) Potential carbon emissions dominated by carbon dioxide from thawed permafrost soils. *Nat Clim Change*. doi:[10.1038/nclimate3054](https://doi.org/10.1038/nclimate3054)
- Schaedel C, Schuur EAG, Bracho R et al (2014) Circumpolar assessment of permafrost C quality and its vulnerability over time using long-term incubation data. *Glob Change Biol* 20:641–652. doi:[10.1111/gcb.12417](https://doi.org/10.1111/gcb.12417)
- Schnecker J, Wild B, Hofhansl F et al (2014) Effects of soil organic matter properties and microbial community composition on enzyme activities in cryoturbated arctic soils. *PLoS ONE* 9:e94076. doi:[10.1371/journal.pone.0094076](https://doi.org/10.1371/journal.pone.0094076)
- Schuur EAG, Bockheim J, Canadell JG et al (2008) Vulnerability of permafrost carbon to climate change: Implications for the global carbon cycle. *Bioscience* 58:701–714. doi:[10.1641/B580807](https://doi.org/10.1641/B580807)
- Schuur EAG, McGuire AD, Schädel C et al (2015) Climate change and the permafrost carbon feedback. *Nature* 520:171–179. doi:[10.1038/nature14338](https://doi.org/10.1038/nature14338)
- Sistla SA, Rastetter EB, Schimel JP (2014) Responses of a tundra system to warming using SCAMPS: a stoichiometrically coupled, acclimating microbe-plant-soil model. *Ecol Monogr* 84:151–170. doi:[10.1890/12-2119.1](https://doi.org/10.1890/12-2119.1)
- Sjögersten S, Caul S, Daniell TJ et al (2016) Organic matter chemistry controls greenhouse gas emissions from permafrost peatlands. *Soil Biol Biochem* 98:42–53. doi:[10.1016/j.soilbio.2016.03.016](https://doi.org/10.1016/j.soilbio.2016.03.016)
- Soil Survey Staff, Natural Resources Conservation Service, United States Department of Agriculture (2015) Soil Survey Geographic (SSURGO) Database. <https://sdmdata.access.sc.egov.usda.gov>. Accessed 9 Sept 2015
- Stephens PA, Buskirk SW, Hayward GD, Martinez del Rio C (2005) Information theory and hypothesis testing: a call for pluralism. *J Appl Ecol* 42:4–12. doi:[10.1111/j.1365-2664.2005.01002.x](https://doi.org/10.1111/j.1365-2664.2005.01002.x)
- Swenson SC, Lawrence DM (2012) Improved simulation of the terrestrial hydrological cycle in permafrost regions by the Community Land Model. *J Adv Model Earth Syst*. doi:[10.1029/2012MS000165](https://doi.org/10.1029/2012MS000165)
- Tang JY, Riley WJ (2013) A total quasi-steady-state formulation of substrate uptake kinetics in complex networks and an example application to microbial litter decomposition. *Biogeosciences*. doi:[10.5194/bg-10-8329-2013](https://doi.org/10.5194/bg-10-8329-2013)
- Tarnocai C (1993) Sampling frozen soils. In: Carter MR (ed) *Soil sampling and methods of analysis*. Lewis Publishers, Boca Raton, pp 755–765
- Tarnocai C, Canadell JG, Schuur E (2009) Soil organic carbon pools in the northern circumpolar permafrost region. *Global Biogeochem Cycles*. doi:[10.1029/2008GB003327](https://doi.org/10.1029/2008GB003327)
- Treat CC, Natali SM, Ernakovich J et al (2015) A pan-Arctic synthesis of CH<sub>4</sub> and CO<sub>2</sub> production from anoxic soil incubations. *Glob Change Biol* 21:2787–2803. doi:[10.1111/gcb.12875](https://doi.org/10.1111/gcb.12875)
- Trivedi P, Anderson IC, Singh BK (2013) Microbial modulators of soil carbon storage: integrating genomic and metabolic knowledge for global prediction. *Trends Microbiol* 21:641–651. doi:[10.1016/j.tim.2013.09.005](https://doi.org/10.1016/j.tim.2013.09.005)
- Tveit AT, Urich T, Frenzel P, Svenning MM (2015) Metabolic and trophic interactions modulate methane production by Arctic peat microbiota in response to warming. *Proc Natl Acad Sci USA* 112:E2507–E2516. doi:[10.1073/pnas.1420797112](https://doi.org/10.1073/pnas.1420797112)
- van Hees PAW, Jones DL, Finlay R et al (2005) The carbon we do not see—the impact of low molecular weight compounds on carbon dynamics and respiration in forest soils: a review. *Soil Biol Biochem* 37:1–13. doi:[10.1016/j.soilbio.2004.06.010](https://doi.org/10.1016/j.soilbio.2004.06.010)
- Vaughan DG, Comiso JC, Allison I, et al (2013) Observations: cryosphere. In: Stocker TF, Qin D, Plattner G-K, Tignor M, Allen SK, Boschung J, Nauels A, Xia Y, Bex V, Midgley PM (eds) *Climate change the physical science basis. Contribution of working group I to the fifth assessment report of the intergovernmental panel on climate change*. Cambridge, UK, University Press and New York, NY, USA, 1535 p
- Wachinger G, Fiedler S, Zepp K et al (2000) Variability of soil methane production on the micro-scale: spatial association with hot spots of organic material and Archaeal populations. *Soil Biol Biochem* 32:1121–1130
- Wagner D, Gattinger A, Embacher A et al (2007) Methanogenic activity and biomass in Holocene permafrost deposits of the Lena Delta, Siberian Arctic and its implication for the global methane budget. *Glob Change Biol* 13:1089–1099. doi:[10.1111/j.1365-2486.2007.01331.x](https://doi.org/10.1111/j.1365-2486.2007.01331.x)
- Waldrop MP, Wickland KP, White RI et al (2010) Molecular investigations into a globally important carbon pool: permafrost-protected carbon in Alaskan soils. *Glob Change Biol* 16:2543–2554. doi:[10.1111/j.1365-2486.2009.02141.x](https://doi.org/10.1111/j.1365-2486.2009.02141.x)
- Wallenstein MD, Burns RG (2011) Ecology of extracellular enzyme activities and organic matter degradation in soil: a complex community-driven process. In: *Methods of soil enzymology*. Soil Science Society of America, pp 1–22
- Wallenstein MD, McMahon SK, Schimel JP (2009) Seasonal variation in enzyme activities and temperature sensitivities in Arctic tundra soils. *Glob Change Biol* 15:1631–1639. doi:[10.1111/j.1365-2486.2008.01819.x](https://doi.org/10.1111/j.1365-2486.2008.01819.x)
- Werner JJ, Koren O, Hugenholtz P et al (2011) Impact of training sets on classification of high-throughput bacterial 16s rRNA gene surveys. *ISME J* 6:94–103. doi:[10.1038/ismej.2011.82](https://doi.org/10.1038/ismej.2011.82)
- Westermann P, Ahring BK (1987) Dynamics of methane production, sulfate reduction, and denitrification in a permanently waterlogged alder swamp. *Appl Environ Microbiol* 53:2554–2559
- Wieder WR, Grandy AS, Kallenbach CM et al (2015) Representing life in the Earth system with soil microbial functional traits in the MIMICS model. *Geosci Model Dev* 8:1789–1808. doi:[10.5194/gmd-8-1789-2015](https://doi.org/10.5194/gmd-8-1789-2015)
- Wild B, Gentsch N, Čapek P et al (2016) Plant-derived compounds stimulate the decomposition of organic matter in arctic permafrost soils. *Sci Rep*. doi:[10.1038/srep25607](https://doi.org/10.1038/srep25607)
- Zuur AF, Ieno EN, Elphick CS (2009) *A protocol for data exploration to avoid common statistical problems*. *Methods Ecol Evol* 1:3–14. doi:[10.1111/j.2041-210X.2009.00001.x](https://doi.org/10.1111/j.2041-210X.2009.00001.x)